Inorganic Chemistry

ARTICLE

pubs.acs.org/IC

# Crystal Structure and Spectroscopic Studies of a Stable Mixed-Valent State of the Hemerythrin-like Domain of a Bacterial Chemotaxis Protein

Akira Onoda,[*,†,‡] Yasunori Okamoto,[†] Hiroshi Sugimoto,[§] Yoshitsugu Shiro,[§] and Takashi Hayashi[*,†]

[†]Department of Applied Chemistry and [‡]Frontier Research Base for Global Young Researchers, Graduate School of Engineering, Osaka University, Suita, Osaka 565-0871, Japan

[§]Biometal Science Laboratory, RIKEN SPring-8 Center, Sayo, Hyogo 679-5148, Japan

Supporting Information

**ABSTRACT:** The bacterial chemotaxis protein of *Desulfovibrio vulgaris* DcrH (DcrH-Hr) functions as an $O_2$-sensing protein. This protein has a hemerythrin-like domain that includes a nonheme diiron center analogous to the diiron center of the hemerythrin (Hr) family. Interestingly, the $O_2$ affinity of DcrH-Hr is $3.3 \times 10^6$ $M^{-1}$, a value 25-fold higher than that of the *Pectinaria gouldii* Hr. This high affinity arises from the fast association of the $O_2$ ligand with DcrH-Hr ($k_{on}$ = $5.3 \times 10^8$ $M^{-1}$ $s^{-1}$), which is made possible by a hydrophobic tunnel that accelerates the passage of the $O_2$ ligand to the diiron site. Furthermore, the autoxidation kinetics indicate that the rate of autoxidation of DcrH-Hr is 54-fold higher than that of *P. gouldii* Hr, indicating that the oxy form of DcrH-Hr is not stable toward autoxidation. More importantly, a mixed-valent state, semimet$_R$, which was spectroscopically observed in previous Hr studies, was found to be stable for over 1 week and isolable in the case of DcrH-Hr. The high-resolution crystal structures of the semimet$_R$- (1.8 Å) and met-DcrH-Hr (1.4 Å) indicate that the semimet$_R$- and met-DcrH-Hr species have very similar coordination geometry at the diiron site.

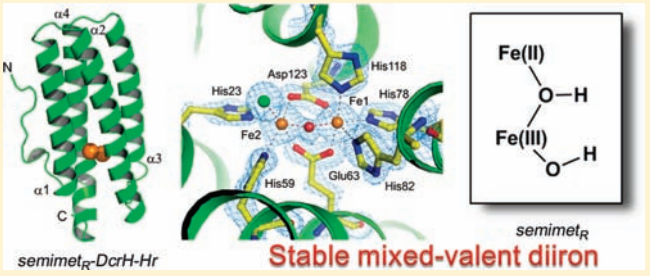


## INTRODUCTION

The diiron center is found among a vast range of metalloproteins that are often involved in reactions with dioxygen. Hemerythrin (Hr) and myohemerythrin are nonheme iron-containing oxygen-transport proteins that were first characterized as dinuclear metalloproteins.[1−5] These proteins have been isolated only from a few phyla of marine invertebrates. The native quaternary structures of these proteins are mostly octamers, although tetramers, trimers, and dimers, as well as monomers are also known. Despite the differences in quaternary structure, the molecular weight of most of the subunits is approximately 13 kDa. One characteristic feature of these proteins is that they have a four-helix bundle structure with five histidine imidazoles and bridging carboxylate groups coordinating to the diiron site with an oxo/hydroxo bridge (Figure 1). One of the two irons in the five-coordinate ferrous center reversibly binds dioxygen.

The diiron site of the Hr proteins exists in the following three oxidation states: [$Fe^{III}Fe^{III}$] in the oxy form and met form, [$Fe^{II}Fe^{II}$] in the deoxy form, and [$Fe^{II}Fe^{III}$] in the semimet form.[3,4,6,7] Deoxy-Hr can be prepared by reduction of met-Hr, which further produces oxy-Hr upon addition of $O_2$. The oxy form is autoxidized to the stable met form. It has also been found that one-electron oxidation of the deoxy form or one-electron reduction of the met form produces two kinds of mixed-valent semimet intermediates between the deoxy form and the met form. Although the mixed-valent diiron core of the Hr proteins has been well-characterized by a variety of spectroscopic methods, the isolation of this intermediate has not been reported because the mixed-valent forms were found to undergo rapid disproportionation to the deoxy and met forms.[6]

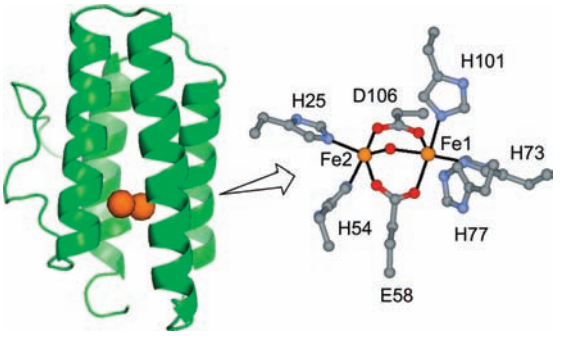


**Figure 1.** Ribbon diagram of hemerythrin and the diiron active site (PDB ID: 1HMD).

Recently, examples of Hr-like domains have been discovered in microorganisms, which is of great interest from the viewpoint

**Received:** January 19, 2011
**Published:** April 29, 2011

  

of similarities in structure and function between different phyla.[8,9] Kurtz and co-workers first reported that DcrH proteins include a Hr-like domain[8] and characterized the recombinant 136-residue DcrH-Hr domain as a soluble and stable monomer containing a diiron site. The diiron site of DcrH-Hr was found to have spectroscopic properties similar to the reported Hr proteins with the $O_2$-binding function, whereas the oxy form of DcrH-Hr is rapidly autoxidized to the met form relative to Hr. On the basis of the striking difference in stability of the oxy form, the DcrH-Hr domain has been proposed to function as an $O_2$ sensor rather than as an $O_2$ binding unit.[8,10] In addition, crystal structural analyses of met-, azidomet-, and deoxy-DcrH-Hr revealed that this domain contains a large ligand-binding tunnel which leads to the five-coordinate Fe2 site.[10] This tunnel is believed to accelerate the process of $O_2$ binding. In this paper, we will describe the detailed kinetic parameters of $O_2$ binding and stability of the mixed-valent state of the DcrH-Hr diiron core as well as the role of the ligand-binding tunnel located adjacent to the diiron site.

## EXPERIMENTAL SECTION

**Materials.** *Desulfovibrio vulgaris* genomic DNA (ATCC 29579D) was purchased from the American Type Culture Collection. Oligonucleotides were obtained from Invitrogen, Inc. Restriction enzymes were obtained from Takara Bio Inc. Nucleotide sequences were determined by GeneDesign, Inc. All reagents of the highest guaranteed grade were purchased and used as received unless otherwise noted. A standard iron solution for inductively coupled plasma optical emission spectroscopy (ICP-OES) was purchased from Nakalai Tesque. Distilled water was demineralized by a Barnstead NANOpure DIamond apparatus.

**Instruments.** The UV−vis experiments were conducted using a Shimadzu UV-3150 double-beam spectrophotometer equipped with a thermostated cell holder with a 0.1 °C deviation. Purification of the proteins was performed using a GE Healthcare ÄKTA Purifier system at 4 °C. The mass analysis of DcrH-Hr protein was carried out using an ESI-TOF MS on an Applied Biosystems Mariner API-TOF workstation. Kinetic measurements of $O_2$ binding were carried out using a stopped-flow/laser-flash photolysis system constructed by Unisoku, Co., Ltd. (Osaka, Japan). A Xe arc lamp was employed as the source of the probe light to follow the spectral changes. For laser-flash photolysis, a sample was excited with 5 ns pulses (532 nm) from a Q-switched Nd:YAG laser (Surelite I, Continuum). ICP-OES was performed on a Shimadzu ICPS-8100. The pH values were monitored with a Horiba F-52 pH meter. Air-sensitive manipulations were performed in an MBraun glovebox.

**Expression and Purification of the DcrH-Hr Domain.** *D. vulgaris* genomic DNA was used as template for PCR with oligonucleotide primers (i) 5′-TATAccatggGTGACGCGGATGTGCTCGTG-3′ and (ii) 5′-GCggatccTCA GGAGACTCCGCGTTCGCGC-3′. The PCR product was digested with *Nco*I and *Bam*HI and ligated with *Nco*I-, *Bam*HI-digested pET16b (Novagen, Inc.). DNA sequencing was performed to verify correct insertion of the gene sequence into the expression vector. The resulting expression plasmid, pET-DcrH-Hr, was transformed into *Escherichia coli* BL21(DE3). Each 1 L of LB medium containing ampicillin (50 mg) and 1% (v/v) glucose was inoculated with an overnight culture (20 mL) of the relevant transformed cells. After the cells were grown aerobically with vigorous shaking at 37 °C until the $OD_{600}$ reached ∼1, isopropyl $\beta$-D-1-thiogalactopyranoside (IPTG) was added to a final concentration of 0.4 mM to induce protein expression. The incubation was continued at 37 °C for approximately 4 h. The cells were harvested by centrifugation at 4000*g* for 10 min. Tricine SDS−PAGE analysis showed that both the supernatant and pellet from the lysed cells contained an overexpressed protein (∼16 kDa).

The harvested cells from 3 L of culture were resuspended in ca. 100 mL of 20 mM Tris-HCl buffer (pH 8.0) and cell lysed by freeze−thaw cycles, followed by a reaction with 10 $\mu$L of benzonase nuclease (Novagen) for 40 min at 25 °C. The lysate was then centrifuged and the collected supernatant was dialyzed three times against 1 L of 20 mM Tris-HCl buffer (pH 8.0). The dialyzed solution was loaded onto an anion-exchange column with DEAE Sepharose Fast Flow (GE Healthcare) which was pre-equilibrated in 20 mM Tris-HCl (pH 8.0). The flow-through fraction of 150 mL containing DcrH-Hr was collected and concentrated to 5 mL using an Amicon stirred ultrafiltration cell with a 10-kDa molecular weight cutoff membrane (Millipore). The sample solution was again loaded onto a HiTrap Q anion-exchange column, and a 35-mL flow-through fraction was collected. The sample fraction was concentrated to 5 mL and exchanged into a buffer containing 200 mM NaCl. This sample was loaded onto a Sephacryl S-200 column (GE Healthcare) equilibrated in the same buffer. The purified fractions were characterized as semimet$_R$-DcrH-Hr as discussed below.

**Preparation of Met- and Deoxy-DcrH-Hr Proteins.** Semimet$_R$-DcrH-Hr was oxidized by addition of at least 10 equiv of potassium ferricyanide at 4 °C for 16 h and the resulting met-DcrH-Hr was purified using a HiTrap desalting column (GE Healthcare) equilibrated with 20 mM Tris-HCl, 200 mM NaCl (pH 8.0).

Semimet$_R$-DcrH-Hr (0.2 mM) was anaerobically reduced by 4 mM sodium dithionite (20 equiv) and 1 mM methylviologen (5 equiv) at room temperature for 3 h, and deoxy-DcrH-Hr was purified using the HiTrap desalting column (GE Healthcare) equilibrated with buffer (20 mM Tris-HCl (pH 8.0), 200 mM NaCl) in the glovebox.

**Crystallization and Structural Analysis.** Crystals of semimet$_R$- and met-DcrH-Hr were grown by hanging drop vapor diffusion by mixing 1.5 $\mu$L of a protein solution with 0.5 $\mu$L of the reservoir solution [0.1 M Tris-HCl (pH 8.5), 12% (v/v) 2-propanol, 26% (w/v) PEG4000, 0.2 M $CaCl_2$] at 4 °C. The crystals were soaked in a cryoprotectant solution (20% ethylene glycol in a reservoir solution) and flash-frozen in liquid nitrogen. The X-ray diffraction data were collected on the BL26B1 beamline at SPring-8, Hyogo, Japan. The data were integrated and merged using HKL2000.[11] The data collection and refinement statistics are listed in Table 1. The initial phases of semimet$_R$-DcrH-Hr and met-DcrH-Hr were obtained by the molecular replacement method using the reported met-DcrH-Hr structure (PDB ID: 2AWY) as a search model. The simulated annealing algorithm of the CNS program[12] was used in the initial stage of structure refinement. After several cycles of manual adjustment with Coot[13] and crystallographic refinement with REFMAC5,[14] water molecules were included. The Fe1−Fe2 distance was not restrained in the refinement. A slight noncrystallographic symmetry restraint was applied to the two monomers in the asymmetric unit. The optical absorption spectra of the single-crystals were measured using a USB2000 fiber optics spectrometer (Ocean Optics). Figures depicting the DcrH-Hr were prepared with PYMOL.[15] The atomic coordinates and structure factors (3AGT and 3AGU) have been deposited into the Protein Data Bank, http://www.rcsb.org/.

**EPR Measurements.** X-band EPR spectra were recorded (9.50 GHz; modulation frequency 100 kHz, modulation amplitude 5G) on a Bruker EMX Plus spectrometer equipped with a cylindrical TE011 cavity. The DcrH-Hr samples were loaded into EPR tubes and quickly frozen in a cold 2-propanol bath chilled with liquid nitrogen. During EPR measurements, the sample temperature was maintained at 5 K by an Oxford Instruments continuous liquid helium cryostat equipped with a turbo pump to lower the vapor pressure of the liquid helium.

**Kinetic Analysis.** Kinetic studies were carried out in 20 mM Tris-HCl (pH 8.0) solution at 20 °C. $O_2$ association for deoxy-DcrH-Hr was measured by monitoring the absorbance changes at 380 and 500 nm after excitation of the oxy form by laser-flash photolysis ($\lambda_{ex}$ = 532 nm, 5 ns pulse) under atmospheric pressure in air. The deoxy form prepared


dx.doi.org/10.1021/ic2001267 |*Inorg. Chem.* 2011, 50, 4892–4899

**Table 1. Statistics of X-ray Data Collection and Structural Refinements of Met-DcrH-Hr and Semimet$_R$-DcrH-Hr**

| | met-DcrH-Hr | semimet$_R$-DcrH-Hr |
|---|---|---|
| | Data Collection | |
| resolution (Å) | 20−1.4 | 20−1.8 |
| high-resolution shell (Å) | 1.45−1.40 | 1.86−1.80 |
| space group | *P*1 | *P*1 |
| unit cell | *a* = 33.31 Å, *b* = 44.87 Å, *c* = 48.13 Å, α = 95.27°, *β* = 104.20°, *γ* = 90.03° | *a* = 33.43 Å, *b* = 44.90 Å, *c* = 48.08 Å, α = 95.21°, *β* = 103.98°, *γ* = 89.95° |
| wavelength (Å) | 0.84 | 0.90 |
| observed reflections | 192 906 | 87 980 |
| unique reflections | 51 015 | 24 033 |
| $R_{sym}$ [a,b] | 0.064 (0.300) | 0.072 (0.358) |
| completeness (%)[a] | 96.5 (89.7) | 97.4 (95.6) |
| $I/\sigma(I)$ [a] | 18.8 (2.7) | 16.3 (3.2) |
| redundancy [a] | 3.8 (3.3) | 3.7 (3.5) |
| | Refinement | |
| $R_{work}/R_{free}$ [c] | 0.203/0.229 | 0.247/0.292 |
| no. of atoms | 2654 | 2636 |
| average *B* values (Å$^2$) | | |
| protein | 7.2 | 11.3 |
| waters | 17.1 | 19.8 |
| other entities | 6.2 | 8.4 |
| rmsd bond (Å) | 0.014 | 0.010 |
| rmsd angle (deg) | 1.48 | 1.23 |

[a] Numbers in parentheses refer to the highest resolution shell. [b] $R_{sym} = \Sigma_{hkl}\Sigma_i|I_i(hkl) - \langle I(hkl)\rangle|/\Sigma_{hkl}\Sigma_i I_i(hkl)$, where $\langle I(hkl)\rangle$ is the average intensity of the *i* observations. [c] $R_{work} = \Sigma_{hkl}||F_{obs}(hkl)| - |F_{calc}(hkl)||/\Sigma_{hkl}|F_{obs}(hkl)|$. $R_{work}$ is calculated for 95% of reflections used for structure refinement. $R_{free}$ is calculated for the remaining 5% of reflections randomly selected and excluded from refinement.

in the glovebox was loaded onto a gel filtration column (HiTrap Desalting, GE Healthcare), which was pre-equilibrated with air-saturated buffer at 20 °C to yield the oxy form. After the oxy form was directly injected from the column into an optical cell under the atmospheric pressure in air, the $O_2$ association was observed by following the absorbance change at 500 nm by laser-flash photolysis. The kinetic model describing $O_2$ binding is presented in the following scheme.

$$\text{oxy-DcrH-Hr} \xrightarrow{h\nu} \text{deoxy-DcrH-Hr} + O_2 \underset{k_{off}}{\overset{k_{on}}{\rightleftharpoons}} \text{oxy-DcrH-Hr}$$

where free $O_2$ is in excess over deoxy-DcrH-Hr; $k_{on}$ and $k_{off}$ are the $O_2$ dissociation and association rate constants. The time course of the absorbance was analyzed by single-phase kinetics to determine the pseudo-first-order rate constant. The observed rate constant, $k_{obs}$, is given as below.

$$k_{obs} = k_{on}[O_2] + k_{off}$$

$O_2$ dissociation was measured using stopped-flow techniques. For this purpose, an excess of sodium dithionite was used to rapidly reduce the $O_2$ concentration in equilibrium, and then $k_{off}$ was obtained as the rate-determining step. The decay of the characteristic absorption at 500 nm for oxy-DcrH-Hr was analyzed using a first-order rate law in each sodium dithionite concentration. The observed rate constants leveled off with addition of a large excess of sodium dithionite to yield the dissociation rate constant. After the oxy form was mixed with sodium dithionite solution, the spectral changes in the range of 400−700 nm were monitored. The probe light at shorter wavelengths (~360 nm) was cut off with an optical filter (Sigma Koki Co., Ltd.). The kinetic model used is presented in the following scheme.

$$\text{oxy-DcrH-Hr} \underset{k_{on}}{\overset{k_{off}}{\rightleftharpoons}} \text{deoxy-DcrH-Hr} + O_2$$

$$Na_2S_2O_4 + O_2 \xrightarrow{k_{red}} \text{products}$$

where $k_{on}$, $k_{off}$, and $k_{red}$ are the $O_2$ dissociation, association, and dithionite reduction rate constants, respsectively. The observed rate constant, $k_{obs}$, is given as an equation below.

$$k_{obs} = k_{off}k_{red}[Na_2S_2O_4]/(k_{on}[O_2] + k_{red}[Na_2S_2O_4])$$

Autoxidation of oxy-DcrH-Hr was measured by monitoring the spectral changes in the range of 300−700 nm at 2 min intervals at 20 °C. The time course of absorbance at 500 nm was analyzed by first-order kinetics to afford the autoxidation rate.

## RESULTS

**Preparation of the DcrH-Hr Domain.** Overexpressed DcrH-Hr found in the soluble fraction of the lysed-cell pellet of *E. coli* BL21(DE3) was collected and the crude protein was purified using an anion-exchange column followed by a gel filtration column. The crude protein ran as a single band with a molecular weight of 16 kDa on Tricine SDS−PAGE. The corresponding mass numbers of the apoprotein determined by the ESI-TOF MS experiments also confirm that a protein of the desired sequence was prepared. Inductively coupled plasma optical emission spectroscopy (ICP-OES) analysis showed that the as-isolated protein contains approximately 1.8 equiv of iron atoms, indicating that this as-isolated form binds 2 equiv of iron atoms at the inherent diiron site.

The existence of the diiron core in the as-isolated protein was also confirmed by EPR measurements. Previous studies clarified that both [$Fe^{II}Fe^{II}$] in the deoxy form and [$Fe^{III}Fe^{III}$] in the met forms are EPR-silent due to antiferromagnetical coupling of the two Fe ions. Furthermore, one-electron reduction of met-Hr and one-electron oxidation of deoxy-Hr yield semimet$_R$ and semimet$_O$, respectively.[7,16,17] It is known that these forms show characteristic rhombic and axial EPR spectra, respectively.[7] Therefore, only two forms of the mixed-valent diiron site provide the characteristic EPR signals. In the case of the as-isolated form of DcrH-Hr, we observed EPR signals at $g$ = 1.91, 1.88, and 1.66. These values are similar to the reported $g$ values for semimet$_R$-Hr (1.96, 1.88, and 1.66) (Figure 2). In addition, the gently sloping absorption from 300 to 400 nm of the semimet$_R$-DcrH-Hr shown in Figure 3 resembles the reported semimet$_R$ absorption of the Hr proteins.[6,16] This evidence indicates that the as-isolated form of DcrH-Hr contains a mixed-valent diiron core in the semimet$_R$ state. The absorption of semimet$_R$-DcrH-Hr did not change over several weeks at 4 °C. It is known that the mixed-valent species of the Hr proteins are not isolable ($t_{1/2}$ = 5−8 min),[7] while the mixed-valent DcrH-Hr species is remarkably stable.

**Preparation of DcrH-Hr with Different Oxidation States.** Starting from isolated semimet$_R$-DcrH-Hr, we prepared met-,


dx.doi.org/10.1021/ic2001267 |*Inorg. Chem.* 2011, 50, 4892–4899

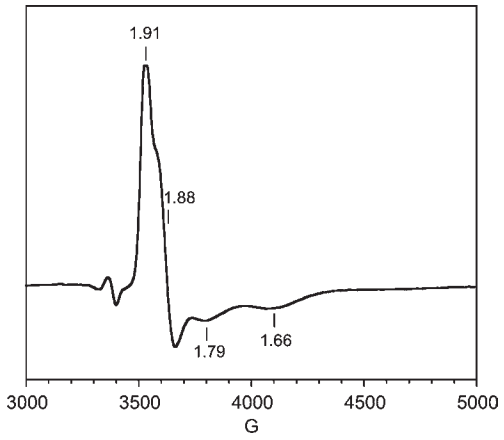


**Figure 2.** X-band EPR spectrum of semimet$_R$-DcrH-Hr (200 $\mu$M) in 20 mM Tris-HCl (pH 8.0) solution containing 100 mM NaCl at 5 K. Instrumental conditions: microwave power, 0.25 mW; modulation frequency, 100 kHz; modulation amplitude, 5 G; sweep rate, 9.54 G/s.

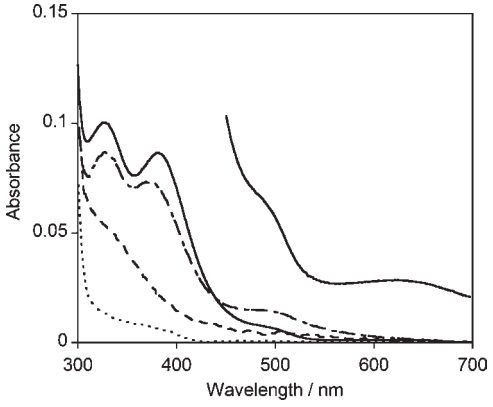


**Figure 3.** UV−vis spectra of met-DcrH-Hr (solid line), semimet$_R$-DcrH-Hr (dashed line), deoxy-DcrH-Hr (dotted line), and oxy-DcrH-Hr (dot-dashed line) in 20 mM Tris-HCl (pH 8.0) solution containing 100 mM NaCl at 20 °C.

deoxy-, and oxy-DcrH-Hr proteins. These derivatives have a diiron core with different oxidation states. It is known that the met-Hrs can be prepared by one-electron oxidation of the semimet$_R$ form.[7,16,17] Treatment of the semimet$_R$-DcrH-Hr form with potassium ferricyanide produced the met form, which has characteristic absorption maxima at 322 and 380 nm and weaker features at near 480 and 620 nm (Figure 3). This spectral profile is consistent with the profile observed for met-Hr.[18] The EPR-silent oxidized form also provides strong evidence of conversion to the met form. Interestingly, when the met-DcrH-Hr sample was analyzed in the ESI MS experiment, we observed the desired mass numbers of holoprotein with two iron atoms connected by a $\mu$-oxo bridge, although the semimet$_R$ form gave the mass numbers of the apoprotein. This difference in MS analyses suggests that the substitution-labile $Fe^{II}Fe^{III}$ core of semimet$_R$ form is eventually dislodged from the protein to give the mass number of the apoprotein during ionization process. In contrast, the met form exhibited the corresponding mass number containing the rigid $Fe^{III}Fe^{III}$ core with the oxo bridge. The corresponding deoxy form of DcrH-Hr was also prepared from the semimet$_R$ form. Reduction of DcrH-Hr proceeds more efficiently with addition of methylviologen, an electron mediator which has been used in the preparation of the reduced form of methane monooxygenase.[19,20] Reduction under anaerobic conditions transformed the mixed-valent $Fe^{II}Fe^{III}$ core into the $Fe^{II}Fe^{II}$ core. This was confirmed by the apparent loss of absorption in the 300−600 nm range. In addition, deoxy-DcrH-Hr reacts with dioxygen to yield the oxy form. This change was clearly observed by the prominent absorption increase at 500 nm, which is assigned to the ligand-to-metal charge-transfer transitions of the $O_2$-bound diferric core observed in other proteins and synthetic complexes.[21,22] The oxy-DcrH-Hr derivative was rapidly autoxidized to the met form, as described previously.[8]

**Crystal Structure of Semimet$_R$-DcrH-Hr.** The X-ray crystal structure of the stable semimet$_R$ form ($Cl^-$-bound form) was determined and refined at 1.8 Å resolution. The semimet$_R$ form of the diiron core in the single crystal was also confirmed by absorption spectroscopy (see Figure S4 in the Supporting Information). The overall structure and the coordination geometry are similar to that of the previously reported met-DcrH-Hr, whose diiron site is buried within the four-helix bundles ($\alpha$1−$\alpha$4) (Figure 4).[10] The two iron atoms are 3.34 Å apart and contain a bridging oxygen atom. There are five histidine and two carboxylic acid residues (aspartic acid and glutamic acid) that act as ligands to the iron atoms. Histidine residues 78, 82, and 112 bind to Fe1 and histidine residues 23 and 59 bind to Fe2. The bridging bidentate carboxylates are provided by Glu63 and Asp123. An exogenous ligand to Fe2 was assigned as chloride, based on the Fe2−Cl distance of 2.4 Å, which is in good agreement with the $Cl^-$-bound met-DcrH-Hr and met-Hr structures in the literature.[10,23,24] To compare the details of the diiron geometries of the semimet$_R$ and met forms, the crystal structure of met-DcrH-Hr was also determined at 1.4 Å resolution and solved using a similar procedure. The superimposed structures of the diiron core in the met and semimet$_R$ forms are shown in Figure 4c. The diiron cores in the two states gave very similar coordination geometry. Since the Fe1−Fe2 distance (3.34 Å) of the semimet$_R$ form became somewhat longer than that of the met form (3.28 Å) in our experiment, the observed difference between the semimet$_R$ and met forms is not statistically significant. Previous model studies reported that the Fe−Fe distances of the $Fe^{II}(\mu$-OH)$Fe^{II}$ and $Fe^{III}(\mu$-OH)$Fe^{III}$ derivatives were longer (+0.2 and +0.29 Å, respectively) than that of $Fe^{III}(\mu$-O)$Fe^{III}$ within a similar ligand environment.[25,26] This indicates that two-electron reduction and/or protonation of the $Fe^{III}(\mu$-O)$Fe^{III}$ entity lead to elongation of the distance between the iron atoms.[25,26] Although an increase of the Fe1−Fe2 distance in the semimet$_R$ form relative to that in met form might be expected, it is within the range of estimated coordinate error (0.18 Å for the semimet$_R$ form and 0.08 Å for the met form).[27]

One of the distinctive features of DcrH-Hr is a putative ligand-binding tunnel leading to the diiron site. This tunnel is not present in the invertebrate Hr proteins. The tunnel is expected to contribute to the rapid autoxidation of DcrH-Hr, which does not occur for the other Hr proteins.[8,29] Mutagenic studies of the Hr proteins have indicated that the rapid autoxidation rate is induced by increased access of water molecules to the diiron site.[23,30] The tunnel is located perpendicular to the long axis of the four-helix bundle in DcrH-Hr and is predominately lined with hydrophobic residues. In the semimet$_R$ form, the tunnel structure was found to be essentially identical to that of the met form. Another characteristic is the different conformation of the N-terminal loop, which occurs when the oxidation state of the diiron site is changed.


dx.doi.org/10.1021/ic2001267 |*Inorg. Chem.* 2011, 50, 4892–4899

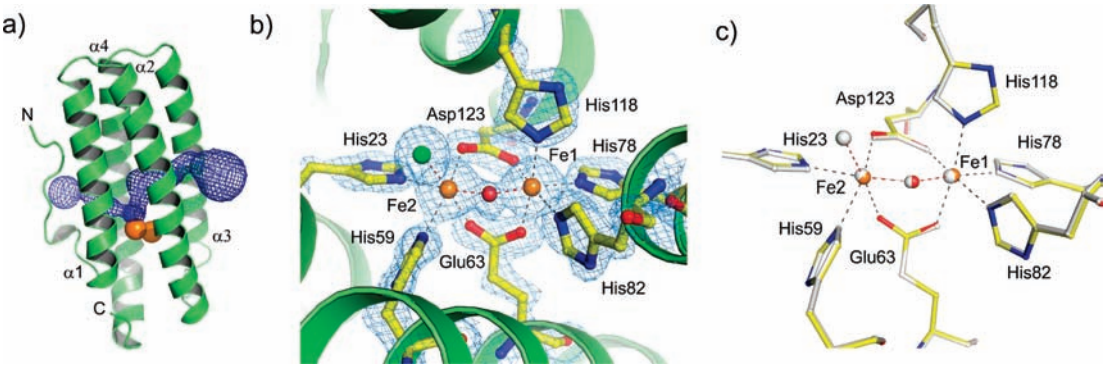


**Figure 4.** (a) Overall structure of semimet$_R$-DcrH-Hr ($Cl^-$-bound form). A blue grid indicates the ligand-binding tunnel (calculated by the CAVER program[28]). (b) The $2F_{obs} - F_{calc}$ electron density in light blue grid (contoured at 1.5 $\sigma$) around the diiron site of semimet$_R$-DcrH-Hr (iron in orange, oxygen in red, nitrogen in blue, and chloride in green). (c) superimposition of the semimet$_R$ (yellow) and met (white) structures.

Previous structural analyses of the met and deoxy forms showed that the N-terminal loop, which includes Trp9, undergoes a conformational change, which has been proposed as the key structural basis for $O_2$ sensing.[10] In contrast, we could not observe the conformational difference between the semimet$_R$ and met forms. This indicates that such a structural change in the loop region is related to reduction from the semimet$_R$ form to the deoxy form.

**Preparation of $Cl^-$-Free Semimet$_R$ and Met Forms.** As-isolated semimet$_R$-DcrH-Hr was found to be in the stable mixed-valent oxidation state. Crystal structural analysis has indicated that this species contains a chloride ion as an exogenous ligand to the Fe2 site. To determine the effect of the binding of $Cl^-$ on the stability of the mixed-valent diiron core in the semimet$_R$ form, we prepared DcrH-Hr with a $Cl^-$-free diiron site. The $Cl^-$-free met form was prepared by buffer exchange with $Cl^-$-free HEPES solution. The absorption spectra of the $Cl^-$-bound met and $Cl^-$-free met forms containing $OH^-$ ligand are shown in Figure 5. The absorption maximum at 382 nm of the $Cl^-$-bound met form shifted to 360 nm for the $Cl^-$-free met form. This result is in good agreement with previous observations of met-Hr proteins. Thus, the buffer exchange procedure apparently removes the $Cl^-$ ion from the diiron site. The $Cl^-$-free semimet$_R$ form was prepared by using a similar method. Although the absorption spectrum of the $Cl^-$-free semimet$_R$ form showed only a slight difference from that of the corresponding $Cl^-$-bound semimet$_R$ form, we observed a significant difference in EPR signals (see Figures S5 and S6 in the Supporting Information). The time course UV−vis analysis suggests that the mixed-valent diiron in the $Cl^-$-free semimet$_R$ form is also stable, although the stability is less than that of the $Cl^-$-bound semimet$_R$ form.

**$O_2$ Binding and Autoxidation Kinetics.** We investigated the inherent $O_2$-binding properties of the diiron core. The kinetic parameters for $O_2$ binding to the $Cl^-$-bound and $Cl^-$-free DcrH-Hrs are summarized in Table 2. The $O_2$ association rate constant, $K_{O_2}$, was determined by monitoring the $O_2$ recombination after cleavage of the Fe−$O_2$ bond by a laser pulse. The profiles obtained at 500 and 380 nm in the laser-flash experiments are shown in Figure 6. The $O_2$ dissociation rate was determined by monitoring the conversion to the deoxy form upon addition of excess amounts of sodium dithionite by stopped-flow techniques (Figure 7). Interestingly, the $O_2$ association rate constant of the DcrH-Hr $Cl^-$-bound form, $5.3 \times 10^8\ M^{-1}\ s^{-1}$, is 160-fold higher than that of *Pectinaria gouldii* Hr, whereas the $O_2$ dissociation rate

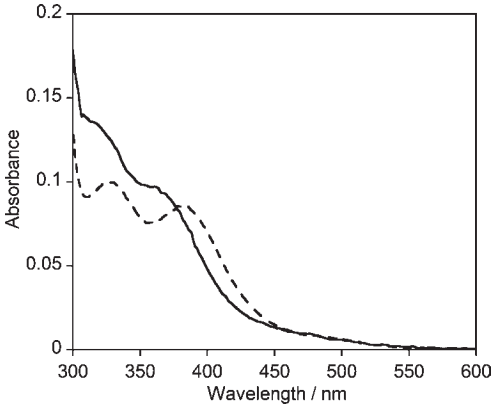


**Figure 5.** UV−vis spectra of the met(OH) form of DcrH-Hr in 20 mM HEPES, pH 8.0 (solid line), and met(Cl) form of DcrH-Hr in 20 mM Tris-HCl, pH 8.0 (dashed line).

of 160 $s^{-1}$ is only 3-fold higher. Thus, the $O_2$ affinity of DcrH-Hr determined from the ratio of the obtained kinetic parameters was found to be increased by 25-fold. This remarkable difference is also found when the kinetic parameters were compared with those of other Hrs reported in the literature. In addition, the 3-fold increase of $k_{on}$ of the $Cl^-$-bound form relative to the $Cl^-$-free form is consistent with the reported evidence that ligation of the chloride ion leads to a 2−4 fold enhancement of $k_{on}$ while having no influence on the $k_{off}$ value in Hr.[31] Furthermore, the autoxidation from oxy to the met form was followed by the characteristic absorption of the oxy form at 500 nm, as shown in Figure 8. The autoxidation kinetics indicate that the autoxidation rate of DcrH-Hr is 54-fold higher than that of *P. gouldii* Hr (Table 2). This indicates that the oxy form of DcrH-Hr is unstable toward autoxidation.

## DISCUSSION

**The Stable Mixed-Valent State of the DcrH-Hr Domain.** Mixed-valent states in the diiron core in the Hr family of proteins have been extensively studied because they are key intermediates between the inactive met form and the active deoxy form. These species are essential for the chemical and structural basis of the reaction cycle that involves binding of $O_2$ to the diiron site, followed by reduction of the met form (Scheme 1). Kinetic


dx.doi.org/10.1021/ic2001267 |*Inorg. Chem.* 2011, 50, 4892–4899

**Table 2. Kinetic Parameters of $O_2$ Binding**

| | $k_{on}$ (x $10^{-6}$ $M^{-1}$ $s^{-1}$) | $k_{off}$ ($s^{-1}$) | $K_{O_2}$ ($M^{-1}$) | $t_{1/2}$[g] |
|---|---|---|---|---|
| DcrH-Hr ($Cl^-$)[a] | 530 | 160 | $3.3 \times 10^6$[e] | 22 min |
| DcrH-Hr ($Cl^-$-free)[b] | 180 | 170 | $1.1 \times 10^6$[e] | 22 min |
| Hr, *P. gouldii* ($Cl^-$-free)[c] | 3.3 | 51 | $1.3 \times 10^5$[f] | 20 h |
| MHr, *Themiste zostericola* ($Cl^-$-free)[d] | 1.4 | 210 | $2.5 \times 10^5$[f] | 19 h |

[a] In 20 mM Tris-HCl, 200 mM NaCl (pH 8.0) at 20 °C. [b] In 20 mM HEPES (pH 8.0) at 20 °C. [c] In 300 mM Tris-sulfate (pH 8.0) at room temperature.[32] [d] In 300 mM Tris-sulfate (pH 8.0) at 21.5 °C.[33] [e] $K_{O_2} = k_{on}/k_{off}$. [f] Calculated from $P_{1/2}$ and $O_2$ solubility. [g] Autoxidation.

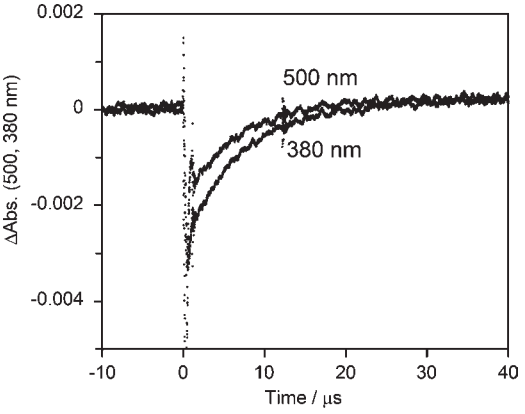


**Figure 6.** Time course of the absorbance at 500 nm after flash photolysis ($\lambda_{ex}$ = 532 nm) of oxy-DcrH-Hr under aerobic conditions. 20 mM Tris-HCl (pH 8.0), 100 mM NaCl at 20 °C, [oxy-DcrH-Hr] = 40 $\mu$M.

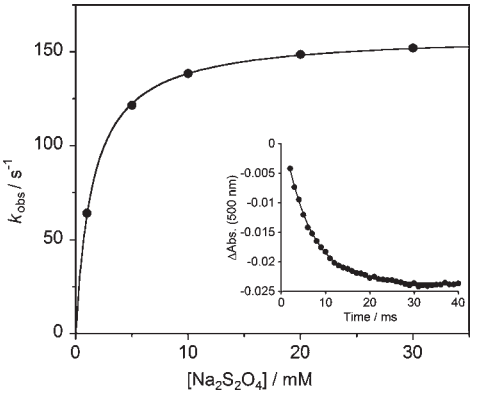


**Figure 7.** Plots of $k_{obs}$ vs sodium dithionite concentration in 20 mM Tris-HCl (pH 8.0) and 100 mM NaCl at 20 °C. [oxy-DcrH-Hr] = 53 $\mu$M (inset, time course of the absorbance at 500 nm over 40 ms. $[Na_2S_2O_4]$ = 45 mM).

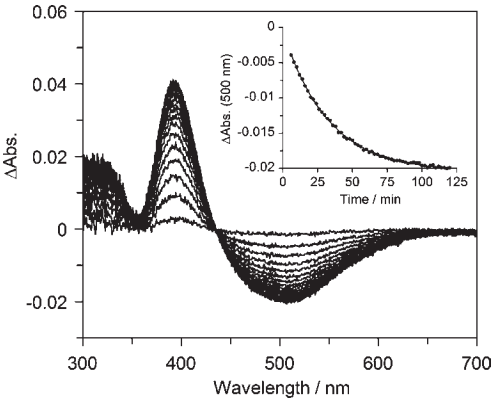


**Figure 8.** Spectral changes of oxy-DcrH-Hr in 20 mM Tris-HCl (pH 8.0) and 100 mM NaCl at 20 °C. [oxy-DcrH-Hr] = 44 $\mu$M (inset, time course of the absorbance at 500 nm).

studies on interconversions between the various oxidation levels of the iron ions within Hr proteins have established the fact that one-electron reduction of the met form yields the semimet$_R$ form and that one-electron oxidation of the deoxy form produces the semimet$_O$ form. The two semimet forms differ with regard to spectroscopic characteristics and reactivity.[3,7,34−36] The semimet$_R$-Hr species is known to be only slowly reduced, but rapidly oxidized to the met form.[7] In contrast, semimet$_O$-Hr is rapidly reduced to the deoxy form, but slowly oxidized. The kinetic studies also suggest that disproportionation could occur via an intramolecular mechanism involving a reaction either with the other binuclear site or with itself.[37] Such a fast disproportionation reaction ($t_{1/2}$ = 5−8 min) leads to the generation of met- and deoxy-Hrs.[6]

To the best of our knowledge, a mixed-valent form of the oxo/hydroxo-bridged diiron core has not been isolated for any of the members of the Hr family of proteins. In contrast, we found that the as-isolated DcrH-Hr protein has a mixed-valent diiron core. In a previous report, Kurtz and co-workers first prepared denatured DcrH-Hr by guanidine hydrochloride, followed by iron incorporation to isolate the holoprotein as the deoxy form.[8] Since they added ferrous ion under the anaerobic condition in the procedure, the purified deoxy form would be converted into the oxy form under the aerobic condition, which is autoxidized to the met form. In the next report, they treated the protein with an excessive amount of potassium ferricyanide before the final purification. Therefore, by these procedures, they isolated the met form, which might be converted from the semimet form.[10] In another paper, Chang and co-workers reported the isolation and characterization of Mc-Hr from *Methylococcus capsulatus* (Bath).[9] They described that the freshly purified met-Mc-Hr, which should normally be an EPR silent species, exhibited EPR signals similar to those of semimet$_R$-Hr and that 22% of the semimet$_R$ form was present in their met form sample. Considering the previous results, the Hr-like proteins found in bacteria would have a stable mixed-valent form, which is well stabilized in the case of DcrH-Hr.

The mixed-valent species in DcrH-Hr can be easily to the met form and to the deoxy form by one-electron oxidation and by one-electron reduction, respectively. This indicates that the as-isolated form is the actual intermediate between the met form and the deoxy form. The oxidation state of the diiron core of the as-isolated DcrH-Hr protein was determined by the characteristic rhombic feature of the EPR signal, which was identical to that of semimet$_R$-Hr. In addition, we analyzed the

**Scheme 1. Plausible Reaction Mechanism of the Diiron Site [Fe1 (upper) and Fe2 (bottom)] in the Hr Family of Proteins**[a]

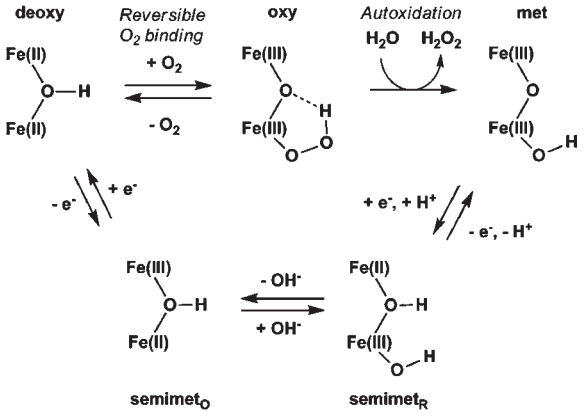


[a] $OH^-$ ligand binds to Fe2. In the case of the DcrH-Hr protein, the semimet$_O$ form is undetectable.

crystal structure of the as-isolated form and identified evidence that the Fe2 ion is hexa-coordinated and includes an exogenous $Cl^-$ ligand. Previous studies on a series of Hr proteins have suggested that conversion from the semimet$_R$ form to the semimet$_O$ form requires dissociation of an exogenous anion ligand from Fe2 and electron transfer from Fe1 to Fe2.[16,17] The observed $Cl^-$ ligand bound to Fe2 in the X-ray crystal structure indicates that the $Cl^-$-bound semimet$_R$-DcrH-Hr was obtained. This exogenous $Cl^-$ ligand can be replaced by buffer exchange to obtain the $Cl^-$-free semimet$_R$ form. This species has an $OH^-$ ligand in place of the $Cl^-$ ligand. However, the stability of the mixed-valent state in the $Cl^-$-free semimet$_R$ form apparently decreased relative to that of the $Cl^-$-bound semimet$_R$ form.

Semimet$_R$-DcrH-Hr was found to be stable enough to isolate as the $Cl^-$ bound form, while the semimet$_O$ form (another mixed-valent state), could not be detected in our experiments. The semimet$_O$ form was reported to be prepared by one-electron oxidation of the deoxy form or by one-electron reduction of the met form at lower pH (pH 6).[17] Although we attempted to prepare the semimet$_O$ form using a similar procedure, the semimet$_R$ form is only detectable by EPR measurements. Thus, semimet$_O$-DcrH-Hr seems to be too unstable to be isolated. In contrast, the instability of Fe(II)Fe(III) mixed-valent form in classical Hr arises from a rapid disproportionation reaction. The previous reports on Hr suggest that the equilibrium between the semimet$_O$ and semimet$_R$ forms promotes the disproportionation. Considering an equilibrium between the semimet$_R$ and the hypothetical semimet$_O$ forms in DcrH-Hr, one of the plausible explanations from our results is that the equilibrium largely shifts to the semimet$_R$ form. Anionic ligands such as $Cl^-$ or $OH^-$, which would coordinate as exogenous ligands, would be expected to be supplied rapidly from a distinct tunnel in the DcrH-Hr protein. The shifted equilibrium is anticipated to greatly reduce the probability to undergo the disproportionation reaction, which leads to the stabilized semimet$_R$ form. In addition, the tunnel would also perturb the conversion from the met form to the semimet$_R$ form. This requires one-electron reduction coupled to protonation of the bridged oxygen atom. The diiron site is thought to be easily exposed to protons contained in the tunnel, which might also shift the equilibrium from the met form to the semimet$_R$ form.

**Increased $O_2$ Association Rate in DcrH-Hr.** The DcrH-Hr domain is proposed to be involved in $O_2$ sensing in the reducing environment of the *D. vulgaris* cytoplasm. Because the diiron core of DcrH-Hr is similar to the typical diiron core of Hr proteins, there is potential for $O_2$ binding. However, the resultant oxy form is rapidly autoxidized to an inactive met form.[8] This is explained by the existence of the ligand binding tunnel linked to the binding site at Fe2, which was demonstrated by the crystal structural analysis.[10] The kinetic analysis of $O_2$ binding to DcrH-Hr indicates that the $O_2$ association rate of DcrH-Hr is faster than the $O_2$ association rates of the Hr proteins, which have been determined in previous reports. In contrast, the $O_2$ dissociation rate is essentially identical to that of the Hr proteins. The results of the quantitative kinetic analysis here support the proposal that the distinct ligand-binding tunnel in DcrH-Hr is advantageous for effective $O_2$ sensing rather than for reversible $O_2$ binding.[10]

**Stable Semimet$_R$ form in Reduction Pathway.** Kurtz and co-workers first characterized DcrH-Hr and proposed that the rationale for the more open binding pocket is to facilitate the rapid autoxidation and that the $O_2$-sensing mechanism of DcrH involves production of hydrogen peroxide, which results in conversion to the met form.[8,10] Likewise, we have demonstrated that the open binding pocket of DcrH-Hr, which is connected to the tunnel, facilitates the binding of exogenous ligands by ca. 10-fold. Given that this process is a reaction for sensing, a reduction pathway from the diferric met form to the diferrous deoxy form is required. The highly reducing intracellular environment of *D. vulgaris* was proposed to provide a reduction pathway for the autoxidized met-from of DcrH in vivo.[10] Considering the efficiency of the reaction cycle, the two-electron reduction of the met form by other redox proteins must produce the deoxy form active for the $O_2$ binding. If the disproportionation reaction competes with this simple pathway, the efficiency of the $O_2$ binding would be decreased, because one of the disproportionation products, the met form, should be reduced again. We anticipate that DcrH-Hr has acquired the ability to prohibit the disproportionation, which leads to the production of the stable mixed-valent form. Even though we successfully isolated the one-electron reduced form, which was characterized as the semimet$_R$ form of DcrH-Hr, the met form is more stable. Thus, the DcrH-Hr domain would be rapidly reduced within the cell via the relatively stable semimet intermediate. It is expected that the tunnel accelerates the conversion of the met form to the corresponding mixed-valent intermediate and eventually contributes to the smooth rereduction cycle. These findings will provide further information for characterizing the detailed $O_2$-sensing mechanism of the oxygen-bridged diiron proteins.

## ■ ASSOCIATED CONTENT

**Supporting Information.** SDS−PAGE analyses for purification, ESI-TOF MS analyses of semimet$_R$- and met-DcrH-Hrs, CD spectra of semimet$_R$- and met-DcrH-Hrs, single crystal absorption spectra of semimet$_R$- and met-DcrH-Hrs. This material is available free of charge via the Internet at http://pubs.acs.org.

## ■ AUTHOR INFORMATION

### Corresponding Author

*Phone: +81-6-6879-7928. Fax: +81-6-6879-7930. E-mail: thayashi@chem.eng.osaka-u.ac.jp.

## ■ ACKNOWLEDGMENT

This work was financially supported by MEXT Japan (A.O. and T.H.), the Frontier Research Base for Global Young Researchers, Osaka University (A.O.), and ATI foundation, Tokyo (A.O.). We acknowledge Dr. Eiichi Mizohata and Prof. Tsuyoshi Inoue at the Department of Applied Chemistry, Graduate School of Engineering, Osaka University, for technical assistance with the protein crystallization, and Dr. Motoyasu Fujiwara at the Research Center for Molecular-Scale Nanoscience, the Institute for Molecular Science (IMS), for technical assistance with EPR measurements.

## ■ REFERENCES

(1) Kurtz, D. M. *J. Biol. Inorg. Chem.* **1997**, *2*, 159–167.
(2) Sazinsky, M. H.; Lippard, S. J. *Acc. Chem. Res.* **2006**, *39*, 558–566.
(3) Wilkins, R. G.; Harrington, P. C. *Adv. Inorg. Biochem.* **1983**, *5*, 51–85.
(4) Wilkins, P. C.; Wilkins, R. G. *Coord. Chem. Rev.* **1987**, *79*, 195–214.
(5) Stenkamp, R. E. *Chem. Rev.* **1994**, *94*, 715–726.
(6) Babcock, L. M.; Bradic, Z.; Harrington, P. C.; Wilkins, R. G.; Yoneda, G. S. *J. Am. Chem. Soc.* **1980**, *102*, 2849–2850.
(7) Muhoberac, B. B.; Wharton, D. C.; Babcock, L. M.; Harrinton, P. C.; Wilkins, R. G. *Biochim. Biophys. Acta* **1980**, *626*, 337–345.
(8) Xiong, J. J.; Kurtz, D. M.; Ai, J. Y.; Sanders-Loehr, J. *Biochemistry* **2000**, *39*, 5117–5125.
(9) Kao, W. C.; Wang, V. C. C.; Huang, Y. C.; Yu, S. S. F.; Chang, T. C.; Chan, S. I. *J. Inorg. Biochem.* **2008**, *102*, 1607–1614.
(10) Isaza, C. E.; Silaghi-Dumitrescu, R.; Iyer, R. B.; Kurtz, D. M.; Chan, M. K. *Biochemistry* **2006**, *45*, 9023–9031.
(11) Otwinowski, Z.; Minor, W. *Macromol. Crystallogr., Pt. A* **1997**, *276*, 307–326.
(12) Brunger, A. T.; Adams, P. D.; Clore, G. M.; DeLano, W. L.; Gros, P.; Grosse-Kunstleve, R. W.; Jiang, J. S.; Kuszewski, J.; Nilges, M.; Pannu, N. S.; Read, R. J.; Rice, L. M.; Simonson, T.; Warren, G. L. *Acta Crystallogr. D* **1998**, *54*, 905–921.
(13) Emsley, P.; Lohkamp, B.; Scott, W. G.; Cowtan, K. *Acta Crystallogr. D* **2010**, *66*, 486–501.
(14) Murshudov, G. N.; Vagin, A. A.; Dodson, E. J. *Acta Crystallogr. D* **1997**, *53*, 240–255.
(15) DeLano, W. L. *The PyMOL Molecular Graphics System*; DeLano Scientific: San Carlos, CA, 2008.
(16) Pearce, L. L.; Kurtz, D. M.; Xia, Y. M.; Debrunner, P. G. *J. Am. Chem. Soc.* **1987**, *109*, 7286–7293.
(17) McCormick, J. M.; Solomon, E. I. *J. Am. Chem. Soc.* **1990**, *112*, 2005–2007.
(18) Garbett, K.; Darnall, D. W.; Klotz, I. M.; Williams, R. J. P. *Arch. Biochem. Biophys.* **1969**, *135*, 419–434.
(19) Fox, B. G.; Froland, W. A.; Dege, J. E.; Lipscomb, J. D. *J. Biol. Chem.* **1989**, *264*, 10023–10033.
(20) Fox, B. G.; Surerus, K. K.; Münck, E.; Lipscomb, J. D. *J. Biol. Chem.* **1988**, *263*, 10553–10556.
(21) Kurtz, D. M. *Chem. Rev.* **1990**, *90*, 585–606.
(22) Solomon, E. I.; Tuczek, F.; Root, D. E.; Brown, C. A. *Chem. Rev.* **1994**, *94*, 827–856.
(23) Martins, L. J.; Hills, C. P.; Ellis, W. R. *Biochemistry* **1997**, *36*, 7044–7049.
(24) Farmer, C. S.; Kurtz, D. M.; Liu, Z. J.; Wang, B. C.; Rose, J.; Ai, J. Y.; Sanders-Loehr, J. *J. Biol. Inorg. Chem.* **2001**, *6*, 418–429.
(25) Armstrong, W. H.; Lippard, S. J. *J. Am. Chem. Soc.* **1984**, *106*, 4632–4633.
(26) Chaudhuri, P.; Wieghardt, K.; Nuber, B.; Weiss, J. *Angew. Chem., Int. Ed.* **1985**, *24*, 778–779.
(27) Cruickshank, D. In *Proceedings of the CCP4 Study Weekend*; SERC Daresbury Laboratory: Warrington, UK, 1996; p 11−22.
(28) Petřek, M.; Otyepka, M.; Banáš, P.; Košinová, P.; Koča, J.; Damborský, J. *BMC Bioinf.* **2006**, *7*, 316.
(29) Xiong, J. J.; Phillips, R. S.; Kurtz, D. M.; Jin, S.; Ai, J. Y.; Sanders-Loehr, J. *Biochemistry* **2000**, *39*, 8526–8536.
(30) Raner, G. M.; Martins, L. J.; Ellis, W. R., Jr. *Biochemistry* **1997**, *36*, 7037–43.
(31) Petrou, A. L.; Armstrong, F. A.; Sykes, A. G.; Harrington, P. C.; Wilkins, R. G. *Biochim. Biophys. Acta* **1981**, *670*, 377–384.
(32) Farmer, C. S.; Kurtz, D. M.; Phillips, R. S.; Ai, J. Y.; Sanders-Loehr, J. *J. Biol. Chem.* **2000**, *275*, 17043–17050.
(33) Lloyd, C. R.; Eyring, E. M.; Ellis, W. R. *J. Am. Chem. Soc.* **1995**, *117*, 11993–11994.
(34) Nocek, J. M.; Kurtz, D. M.; Pickering, R. A.; Doyle, M. P. *J. Biol. Chem.* **1984**, *259*, 2334–2338.
(35) Armstrong, G. D.; Sykes, A. G. *Inorg. Chem.* **1986**, *25*, 3514–3516.
(36) Armstrong, G. D.; Ramasami, T.; Sykes, A. G. *Inorg. Chem.* **1985**, *24*, 3230–3234.
(37) Harrington, P. C.; Wilkins, R. G. *J. Am. Chem. Soc.* **1981**, *103*, 1550–1556.